

# Vehicle Shape Optimisation For Minimization Of Sonic Boom

Chada Sahith Reddy, 180202  
Irene Grace Karot Polson, 180308  
Shrikant Dalmia, 180739  
Simran Singh, 180765

**ABSTRACT.** This report provides an overview of the research done on optimizing supersonic flight and an estimation of the sonic boom generated during supersonic flights. The noise created during the flight due to the sonic boom poses a hurdle to commercializing supersonic transport. Several parameters have to be optimized for a given flight condition to study the sonic boom's minimization. This process involves the minimization of pressure perturbations generated by the aircraft during supersonic flight. These pressure perturbations can be obtained by leveraging linearized analysis with some corrections built-in so that non-linear effects can also be modeled in terms of F-function, as defined by Whitman with the help of numerical methods. We adopted a simplified sonic-boom prediction method to analyse the effects of flight Mach Number on different aircraft geometries.

**Keywords:** aircraft structures, optimization methods, sonic boom, supersonic flight

## INTRODUCTION

When an aircraft passes through the air, it creates a series of pressure waves around its body. These waves travel at the speed of sound, and, as the plane reaches the speed of sound, the waves are forced together, or compressed, because they cannot get out of each other's way quickly enough. Eventually, they merge into a single shock wave, which travels at the speed of sound, a critical speed known as Mach 1, and is approximately 1,235 km/h (767 mph) at sea level and 20 °C (68 °F).

On January 21, 1976, two supersonic planes took flight, one from London and the other from Paris, with speed roughly equal to 1,350 miles per hour (twice the speed of sound). Before this, the sonic boom phenomenon was not explicitly explored. Research through the 1950s and 1960s was focused on understanding the origins of the sonic boom and was marked by the research on weak shock waves and N-wave far-field signatures.

Whitham's [1] classic paper in 1952 described the disturbance produced in the surrounding air by a slender, axisymmetric body moving with supersonic speed. This mathematical theory forms the basis of most of the linearized analysis used in predicting sonic boom near-field. The linearized theory assumed the disturbances to be propagated along parallel characteristic lines. It was observed from experiments that the actual flow field had curved characteristics. Furthermore, a linearized theory cannot predict any shocks because shocks are a highly non-linear phenomenon. So, rather than discard all linearized relations and resort to non-linear analysis, Whitham thought of an ingenious way to use linearized analysis with some corrections built-in so that non-linear effects

can also be modeled. The basic concepts of the improved linearized theory and how F-function is formulated is given below.

**1.1. Improvement of Linearized Theory.** Let the steady stream have velocity  $U$  in the  $x$ -direction, and at a general point  $(x, r)$  let the velocity be  $(U + Uu, UV)$ . The flow is assumed to be irrotational hence the perturbation velocities  $u$  and  $v$  may be deduced from a potential  $\phi$  on the linearized theory, satisfies the equation

$$(1.1) \quad \phi_{rr} + \frac{\phi_r}{r} - \alpha^2 \phi_{xx} = 0$$

where  $\alpha = \sqrt{M^2 - 1}$  and suffixes denote partial differentiation. The solution of 1.1 which represents a disturbance propagated downstream from a body is

$$(1.2) \quad \phi = - \int_0^{x-\alpha r} \frac{f(t)}{\sqrt{(x-t)^2 - \alpha^2 r^2}} dt$$

The arbitrary function  $f(t)$  is determined from the boundary condition on the body that the normal velocity at the body surface is zero. This is further used to define Whitham's F-function,  $F(y)$  defined as

$$(1.3) \quad F(y) = \int_0^y \frac{f'(t)}{\sqrt{y-t}} dt$$

With  $\phi$  and  $F(y)$  now defined by 1.2 and 1.3 parameters such as  $u, v$  and the other parameters which define the shape and structure of the aircraft can be calculated. We have not included the formulations of such parameters in this paper, the interested reader can refer to the concepts laid by Rallabhandi [2] which is an extension of Whitham's theory. With advancement in technology, researchers have been able to provide accurate predictions of the sonic-boom phenomena but the process for obtaining these solutions have become quite complex. One might face the problem mentioned above while following the research done by Rallabhandi to predict said parameters. The method requires one to formulate and run a complex MATLAB code to obtain the program required to run the F-function. Since that process is quite cumbersome due to reasons stated above, we adopt a simplified sonic-boom prediction method provided by Harry W. Carlson [3] which is discussed under Simplified Sonic-Boom Prediction Method.

## BACKGROUND RESEARCH

### 1. WING PLANFORMS AND THEIR EFFECTS ON SONIC BOOM

Ames Research Center [4] conducted a study to investigate the overpressure characteristics of conventional and unconventional wing platform shapes at Mach numbers 1.7, 2.0, 2.7. They studied twelve models under a delta wing series, a swept-wing series, and a curved leading edge wing series in total. The theoretical calculations accounted for some errors due to lift and Mach number effects, which showed considerable deviation from experiments for both near-field (wind tunnel) and mid-field (flight) distance conditions. However, the impact of planform variation was predicted by them reasonably well, these are discussed below.

- (1) **Delta-wing series:** The increase in leading-edge sweep angle (around  $10^\circ$  increase) reduced the maximum overpressure by  $20\%$  at midfield distance ratios for Mach numbers 1.68 and 2.7. In addition to that, they found that tailoring of nose bluntness, body shape, and wing position reduce bow-shock peak pressure (compared to conventional sharp-nosed designs) and arrest the coalescence of the bow and wing shocks.
- (2) **Swept-wing series:** The near-field peak wing overpressure of a swept-wing model with the same wetted area and leading-edge sweep angle (but with a higher aspect ratio and a little less volume) is about  $30\%$  less than that of the delta wing. A similar comparison at midfield distance ratio of 130 shows a difference of about  $10\%$  at Mach number 1.68. At Mach number 2.7, the overpressure for both the wings was very similar.
- (3) **Curved-edge wing series:** The addition of curved strakes to trapezoidal wing and curvature at wingtips did little to weaken the wing shock.

Overall, they concluded that local shape changes of wing platforms obtained with strakes, cranks, or curvatures (like in curved-edge wing series) had little effect on shock-system development. On the other hand, the leading-edge sweep angle changes reduce the magnitude of shock overpressures by about  $20\text{-}40\%$  compared with conventional wing platform designs. Additionally, eliminating the straight edges on leading and trailing edges through a circular wing has no significant effect on sonic-boom overpressure<sup>1</sup>. Furthermore, they remarked that optimizing a given configuration's aerodynamic efficiency is neither a guarantee nor a valid criterion for achieving a low sonic boom.

## 2. REDUCING THE SONIC BOOM INITIAL PRESSURE RISE

Charbel Farhat [5] worked on the effects of different shape and design parameters on Sonic boom initial pressure rise by using the true geometry for the calculations. He worked on optimizing two different airplane concepts developed by Reno Aeronautical and Lockheed Martin, respectively.

The theories from which the research was continued and improved were the Jones Seebass George Darden (JGSD) sonic boom minimization theory and Whitham's theory. According to the JSGD theory, the lowest ISPR ground signature for an N wave occurs when intermediate shocks and compressions merge into the bow and tail shock as close to the vehicle as possible, with the result that a blunt-nosed vehicle produces a reduced ISPR. This ISPR reduction occurs at the expense of maximum drag. A limitation of the JSGD theory is that it only provides an area distribution. Physical volume and lift distribution contribute to the cross-sectional area distribution of the equivalent body; the distributions defined by the JGSD are not unique.

Hayes and coworkers recognized the possibility of a "frozen" midfield signature at some altitude above the ground. Multiple shocks might be frozen at a relatively high altitude and continue to attenuate before reaching the ground to produce lower shock overpressures.

The study cases considered are provided in Fig. 1. In each case, constant lift (equal to the weight of the POD) was maintained. The results of the study mentioned are as follows-

- (1) **Reno Aeronautical:** The initial shock pressure rise on the ground is reduced by a factor close to 2, from 1.224 psf ( $58:605\text{ N/m}^2$ ) at a freestream Mach number of 1.5 to 0.671 psf ( $32:127\text{ N/m}^2$ )

---

<sup>1</sup>Interested reader may refer APPENDIX C for a note on industry designs opted to reduce sonic boom

- (2) **Lockheed Martin:** A tenfold reduction of the initial shock pressure rise on the ground is demonstrated, from 1.623 psf (77:71  $N/m^2$ ) at a freestream Mach number of 1.5 to 0.152 psf (7:278  $N/m^2$ ).

The future objective is to practically achieve ISPR (on the ground) to be less than 0.3 psf (14:364  $N/m^2$ ).

Shape optimization	$\frac{\Delta G(\Gamma)}{G(\Gamma^0)}$	ISPR Eq. (8)	ISPR (ARAP)
Nose (tilting)	4.5%	1.551 psf (74.262 $N/m^2$ )	1.549 psf (74.166 $N/m^2$ )
Canard (positioning)	4.0%	1.558 psf (74.597 $N/m^2$ )	1.553 psf (74.358 $N/m^2$ )
Canard (dihedral and sweep)	24.9%	1.218 psf (58.318 $N/m^2$ )	1.215 psf (58.175 $N/m^2$ )
Canard and wing (dihedral and sweep)	31.5%	1.111 psf (53.195 $N/m^2$ )	1.107 psf (53.003 $N/m^2$ )
Canard and wing (dihedral, sweep, and twist)	56.0%	0.714 psf (34.186 $N/m^2$ )	0.159 psf (7.613 $N/m^2$ )
Nose (tilting) and canard and wing (dihedral, sweep, and twist)	63.4%	0.594 psf (28.441 $N/m^2$ )	0.152 psf (7.278 $N/m^2$ )

**Figure 1.** Incremental shape optimization of LM's POD supersonic platform

### 3. LIMITATIONS

In the studies we have surveyed so far, increasing the Mach number (close to 2.7) and the addition of lift intensifies the discrepancies between theory and experiment. These discrepancies can be attributed in some measure to the limitations of supersonic lifting theory, JGSD theory, and sonic-boom theory in the near field used. Until models large enough to permit the measurement of the load and pressure distributions are tested, the details of these limitations, in theory, cannot be resolved.

### SIMPLIFIED SONIC-BOOM PREDICTION METHOD

This method is developed for a wide variety of supersonic aircraft configurations operating at altitudes up to 76km. The outlined procedure relies to a great extent on the use of charts to provide generation and propagation factors for use in relatively simple expressions for signature calculation. The effects of flight-path curvature and aircraft acceleration, however, are not considered, and the method is further restricted to a standard atmosphere without winds. These limitations, however, do not appear to affect the general applicability of the method for normal variations from the standard atmosphere and for moderate flight-path curvature and aircraft acceleration. Another assumption is that the pressure signal generated by the aircraft is of the classical N-wave.

The procedure for calculation of sonic boom by the simplified method involves three basic steps: determination of an aircraft shape factor, evaluation of atmospheric propagation factors, and calculation of signature shock strength and duration. These basic steps are implemented as follows:

- (1) Determine aircraft shape factors  $K_s$  using the charts provided in [3] which use aircraft weight and operating conditions to calculate lift parameter and thus  $K_s$  can be read directly.
- (2) Determine propagation parameters  $M_e$  and  $h_e$  from the operating conditions according to equations given in APPENDIX A<sup>2</sup> and read atmospheric factors  $K_p$  and  $K_t$  from the charts discussed in [3].

<sup>2</sup>APPENDIX A defines all the symbols used to define the given equations and additional expressions required for the analysis done in this paper

(3) Calculate Bow-shock overpressure and signature curve duration from the equations,

$$(3.1) \quad \Delta P_{max} = K_p K_R \sqrt{p_v p_g} (M^2 - 1)^{1/8} h e^{-3/4} l^{3/4} K_S$$

$$(3.2) \quad \Delta t = K_t \frac{3.42}{a_v} \frac{M}{(M^2 - 1)^{3/8}} h e^{1/4} l^{3/4} K_S$$

### ANALYSIS

In this report, we have analysed the effect of **Mach Number** and **Altitude** by comparing the maximum bow-shock overpressure and signature curve duration obtained for three different types of air-crafts:

- (1) Delta Wing: McDonnell Douglas F-15 Eagle, Fixed Wing Fighter
- (2) Delta Wing: B-58 Hustler, Medium Bomber
- (3) Swept Wing: F-111F, Variable Sweep Aircraft

The far-field simulation conditions for different aircrafts are illustrated in Table 1. The values of other parameters considered are taken as constants for every case. These are, flight path angle  $\gamma = 0$ , ray-path azimuth angle  $\theta = 0$ , atmospheric pressure at ground level  $p_g = 92.3 \text{ kPa}$ , altitude of ground above sea level  $h_g = 0.760 \text{ km}$ , speed of sound  $a_v = 295 \text{ m/sec}$ , and reflection factor  $K_R = 2.0$ .

**Table 1.** Near-field simulation conditions for different aircrafts.

Aircraft Type	Wing Planform	Altitude (km) $h_e$	Standard Pressure (kPa) $p_v$	Mach Numbers $M$
F-15	Delta Wing	15.240	11.6	1.2, 2, 2.5, 3, 4
B-58	Delta Wing	15.240	11.6	1.2, 2, 2.5, 3, 4
F-111F	Swept Wing	15.240	11.6	2, 2.5, 3, 4

We also carried out calculations for B-70 Delta Wing aircraft corresponding to a Mach number of 1.5 and at an altitude of 15.240 km. The value of  $K_L \approx 0.14$  corresponding to which, the value of  $K_S$  could not be obtained from the charts given in [3]. The results obtained for aircrafts described in Table 1 are shown in Tables 2-5 and Figures 2-6.

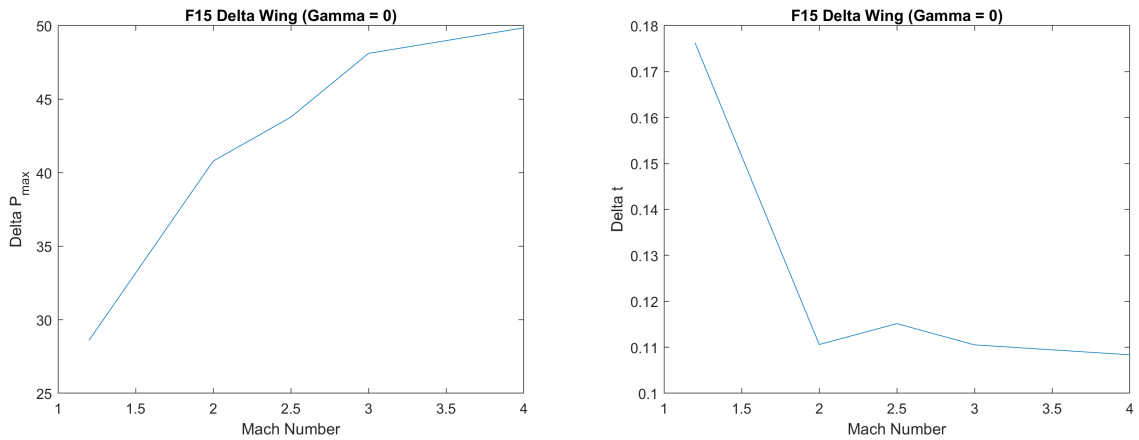
**Table 2.** Variation of ground overpressure of F-111F at M=2

Altitude (km) $h_e$	Standard Temperature ( $^{\circ}\text{C}$ ) $T$	Standard Pressure (kPa) $p_v$	$\Delta P_{max}$ $Pa$	$\Delta t$ $sec$
15	-56.5	12.11	46.326016	0.120921
20	-56.5	5.529	24.977840	0.130369
25	-51.6	2.549	14.261685	0.136552
30	-46.64	1.197	8.490816	0.141562
40	-22.8	0.287	3.334491	0.144924
50	-2.5	0.07978	1.482838	0.147518
60	-26.13	0.02196	0.677236	0.161723
70	-53.57	0.0052	0.293169	0.178358
80	-74.51	0.0011	0.121863	0.193963

**Table 3.** Results for F-15, Fixed Wing Fighter, Delta Wing

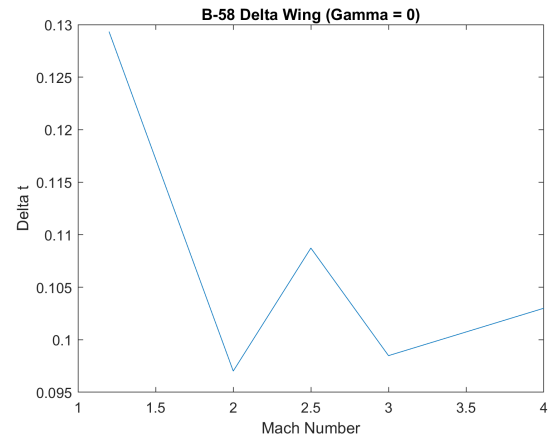
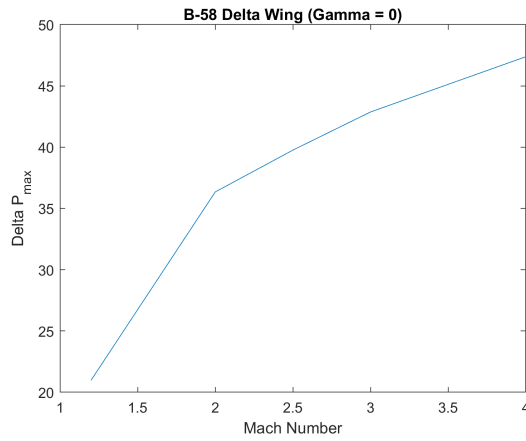
Mach Number $M$	$\Delta P_{max}$ $Pa$	$\Delta t$ $sec$
1.2	28.582626	0.1762532
2	40.792051	0.110602
2.5	43.779767	0.115154
3	48.113614	0.110526
4	49.851394	0.108367

F-15


**Figure 2:** Variation of  $\Delta P_{max}$  and  $\Delta t$  with Mach Number, for F-15.

**Table 4.** Results for B-58, Medium Bomber, Delta Wing

Mach Number $M$	$\Delta P_{max}$ $Pa$	$\Delta t$ $sec$
1.2	20.9740784	0.129335
2	36.347721	0.0970163
2.5	39.760114	0.108729
3	42.872	0.098484
4	47.381	0.102997

**Figure 3:** Variation of  $\Delta P_{max}$  and  $\Delta t$  with Mach Number, for B-58.**Table 5.** Results for F-111F, Variable Sweep Aircraft

Mach Number $M$	$\Delta P_{max}$ $Pa$	$\Delta t$ $sec$
2	44.775242	0.121402
2.5	48.978827	0.119298
3	52.811730	0.121319
4	58.367144	0.126878

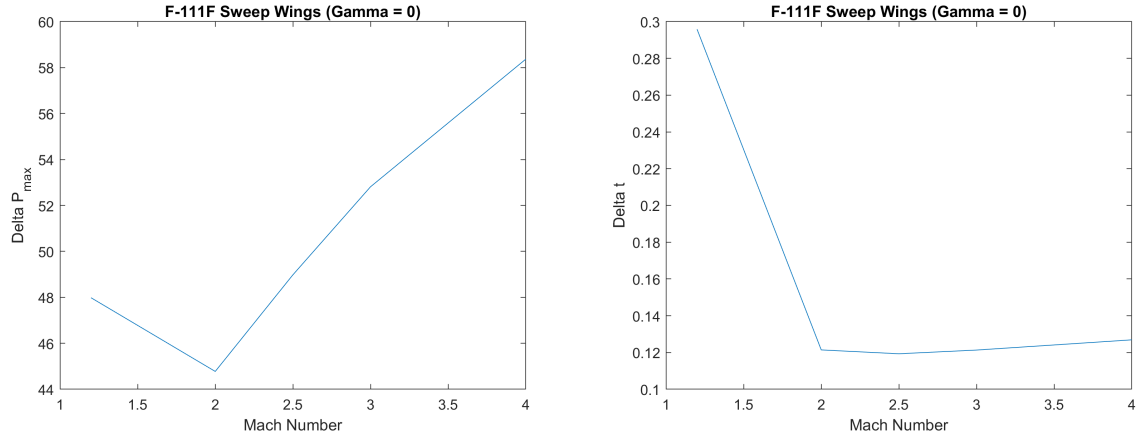


**Figure 4:** Variation of  $\Delta P_{max}$  and  $\Delta t$  with Mach Number, for F-111F.

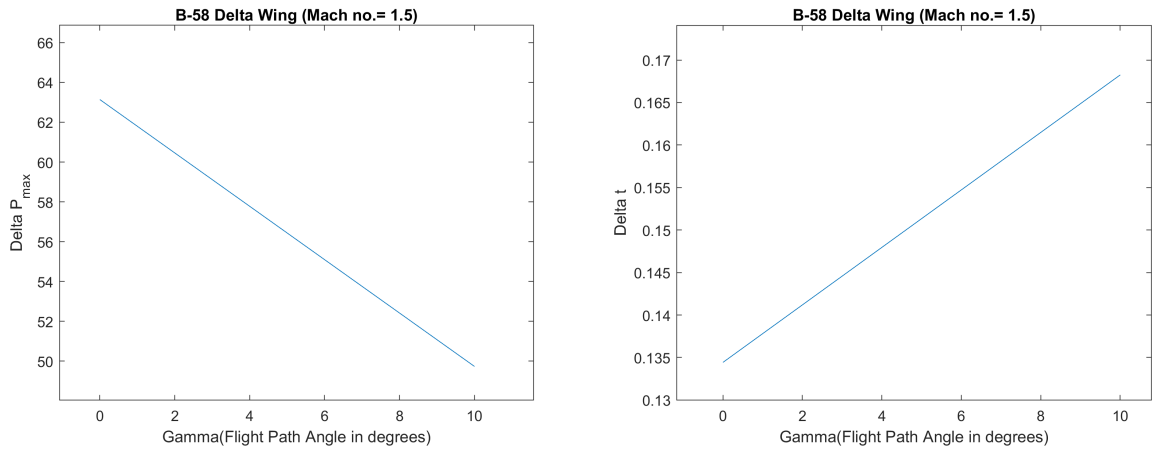


**Figure 5:** Variation of  $\Delta P_{max}$  and  $\Delta t$  with Flight Path Angle for B-58.

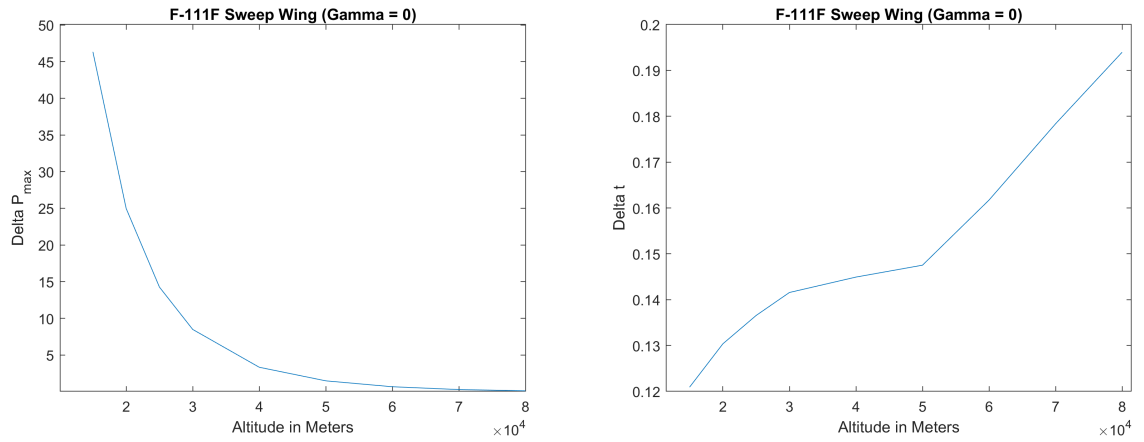


**Figure 6:** Variation of  $\Delta P_{max}$  and  $\Delta t$  with Altitude, at M=2 for F-111F.



### CONCLUSIONS

For the ground sonic boom prediction, near-field domain at the flight altitude 15.240 km is predicted following a simplified method as described in the report. We have carried out the calculations by formulating a MATLAB code which can be viewed in APPENDIX B. We have varied the Mach numbers from 1.2 to 4. The trends obtained by studying the graphs are given below.

- $\Delta P_{max}$  increases with increase in the Mach number for all typed of aircrafts chosen, which can be incurred from Fig. 2. This agrees with the analysis done by Lengyan[6].
- $\Delta P_{max}$  for a given aircraft and a given mach number the effect of increasing altitude can be incurred from Fig. 4. This trend is supported by the equation (3.1) where  $\Delta P_{max} \propto \sqrt{p_v} h e^{-3/4}$ . Therefore, as  $h_e$  increases (which implies decrease in  $p_v$ ), the value of overpressure will decrease. This agrees with the analysis done by Lengyan[6].
- $\Delta t$  decreases with increase in Mach number at a given altitude and increases with increase in altitude at a given Mach number.
- For an increase in Mach number from 2 to 4, F-15(Delta Wing) sees a 22.2% increase in  $\Delta P_{max}$ , whereas for an increase in Mach number from 2 to 2.5, the increase in  $\Delta P_{max}$  is 7.3%.
- For an increase in Mach number from 2 to 4, F-111(Swept Wing) sees a 30.3% increase in  $\Delta P_{max}$ , whereas for an increase in Mach number from 2 to 2.5, the increase in  $\Delta P_{max}$  is 9.4%.
- For an increase in Mach number from 2 to 4, B-58(Delta Wing) sees a 30.36% increase in  $\Delta P_{max}$ , whereas for an increase in Mach number from 2 to 2.5, the increase in  $\Delta P_{max}$  is 9.4%.
- The weight of the B-70 Delta Wing aircraft is too heavy and the calculation of  $K_S$  is not possible. From this we can conclude that there is a limitation to how fast these heavy planes can fly.
- For variation in flight path angle  $\gamma$ , the  $\Delta P_{max}$  decreases as the effective Mach number decreases as shown in the analysis. The trend also shows that  $\Delta t$  increases slightly with  $\gamma$ .

This is in correspondence with the theory that as the aircraft flies with higher speed/Mach number, the impact of the sonic boom over-pressure would increase as well as time taken for the over-pressure difference would decrease making it a stronger sonic boom. Our analysis with the simplified sonic boom prediction thus follow the theoretically established trends.

### REFERENCES

- (1) G. B. Whitham: The Flow Pattern of a Supersonic Projectile. University of Manchester, England. Communications On Pure And Applied Mathematics, VOL. V, 301-348, 1952.
- (2) Sriram Rallabhandi: Sonic Boom Minimization through Vehicle Shape Optimization and Probabilistic Acoustic Propagation. School of Aerospace Engineering Georgia Institute of Technology, April 2005.
- (3) Harry W. Carlson: Simplified Sonic Boom Prediction. Langley Research 1969.
- (4) Lynn W. Hunton, Raymond M. Hicks, Joel P. Mendoxu: Some Effects of Wing Planform on Sonic Boom. NASA Ames Research Center Moffett Field, CA, United States
- (5) Charbel Farhat, Kurt Maute, Brian Argrow, Melike Nikbay: Shape Optimization Methodology for Reducing the Sonic Boom Initial Pressure Rise. AIAA JOURNAL Vol. 45, No.5, May 2007

- (6) Lengyan, Qian Zhansen: A CFD Based Sonic Boom Prediction Method and Investigation on the Parameters Affecting the Sonic Boom Signature, a AVIC Aerodynamics Research Institute, Shenyang, 110034, China.

APPENDIX A

## SYMBOLS AND EQUATIONS

$h$	altitude of aircraft above ground, $h_v - h_g$ , km
$h_e$	effective altitude (see fig. 5), km
$h_g$	altitude of ground above sea level, km
$h_v$	altitude of aircraft (vehicle) above sea level, km
$K_d$	ray-path distance factor
$K_L$	lift parameter
$K_P$	pressure amplification factor
$K_R$	reflection factor, assumed to be 2.0
$K_S$	aircraft shape factor
$K_t$	signature duration factor
$L$	aircraft characteristic length, normally the fuselage length, m
$M$	aircraft Mach number
$M_e$	aircraft effective Mach number governing sonic-boom atmosphere propagation characteristics.
$\Delta P_{max}$	incremental pressure at N-wave bow shock, also referred to as bow-shock overpressure, Pa.
$p_g$	atmospheric pressure at ground level, Pa
$p_v$	atmospheric pressure at aircraft (vehicle) altitude, Pa
$t$	time increment, sec
$W$	aircraft weight, kg
$\gamma$	flight-path angle, degree
$\theta$	ray-path azimuth angle, degree
$\beta$	angle between aircraft ground track and ground projection of ray path, degree

$$M_e = \sqrt{1 + \frac{[A(1 - B \tan \gamma)]^2}{A[\tan \gamma + B]^2 + (CD)^2}}$$

$$\beta = \tan^{-1} \left( \frac{\tan \theta \cos \gamma D}{\tan \gamma + A} \right)$$

$$A = \frac{1}{\cos \gamma \sqrt{M^2 - 1}}$$

$$B = \frac{1}{\cos \theta \sqrt{M^2 - 1}}$$

$$C = \frac{\tan \theta}{\sqrt{M^2 - 1}}$$

$$D = \tan \gamma^2 + 1$$

$$h = h_v - h_g$$

$$d = \frac{K_d h}{\sqrt{M_e^2 - 1}}$$

$$d_x = d \cos \beta$$

$$d_y = d \sin \beta$$

$$h_e = \sqrt{d_y^2 + [h \cos \gamma + d_x \sin \gamma]^2}$$

$$K_L = \frac{\sqrt{M^2 - 1} W \cos \gamma \cos \beta}{(1.4) p_v M^2 l^2}$$

## APPENDIX B

## MATLAB CODE

```

M = 2; %change Mach Number
l = 22; %change Length of Fuselage (metre)
gamma = 0; %change Flight Path Angle (degrees)
theta = 0; %change Ray-Path Angle (degrees)
hv = 15000; %change height above ground (m)
w = 45000; %change weight of Aircraft (kg)
pv = 12110; %atmospheric pressure at aircraft (vehicle) altitude (Pa)
av = 295; %speed of sound at aircraft (vehicle) altitude (m/sec)
hg = 760; %change altitude of ground above sea level (km)
pg = 92300; %atmospheric pressure at ground level (Pa)
kr = 2.0; %reflection factor, assumed to be 2.0
h = hv-hg; %altitude of aircraft above ground, hv - hg (km)

temp = -56.5 + 273;
av = sqrt(1.4*287*temp);

k1 = (sqrt(M^2 - 1)*w*cosd(gamma)*cosd(theta))/(1.4*pv*M^2*l^2);
ks = 0.08; %change from graph with K1
%Or use this for approximate value ks = 0.74*(sqrt(k1 + 0.027))

A = 1/(cosd(gamma) * sqrt(M^2 - 1)) ;
B = 1/(cosd(theta) * sqrt(M^2 - 1)) ;
C = tand(theta)/sqrt(M^2 - 1);
D = (tand(gamma))^2 + 1 ;
phi = atand((tand(theta)*cosd(gamma)*D)/(tand(gamma)+A));

Me = sqrt( 1 + ((A*(1-B*tand(gamma)))^2 / ((A*(tand(gamma)+B))^2 + (C*D)^2));

kd = 1.1; %change from graph for M
d = kd*(h/sqrt(Me^2 - 1));
dx = d*cosd(phi);
dy = d*cosd(phi);
he = sqrt( dy^2 + (h*cosd(gamma) + dx*sind(gamma))^2);

kp = 1.1; %change from graph for M
kt = 0.85; %change from graph for M

delta_Pmax = kp*kr* sqrt(pv*pg) * ((M^2 - 1)^(1/8)) * (he^(-3/4)) * (1)^(3/4) * ks ;

delta_t = kt *(3.42 / av) * (M/(M^2 - 1)^(3/8))* he^(1/4) * 1^(3/4) * ks;

```

## APPENDIX C

### INDUSTRY DESIGNS TO REDUCE SONIC BOOM

**Concorde-** Concorde was designed in the 1960s and early 1970s by the combined efforts of British Aerospace and ONERA. Some of the notable features were its needle-shaped design, the smooth and continuously varying sweep of the wing platform, nacelles placed under the wing, and the absence of a horizontal tail and canard surface. The nose, when dropped down to  $5^\circ$  during take-off and  $12.5^\circ$  during landing, helped improve the pilot's view of the runway. Fly-by-wire controls and stability augmentation systems achieve stability. Simultaneously, transitioning from subsonic to the supersonic regime, the design allowed for fuel motion, which allowed the center of gravity's location to change.

**Gulfstream-** They have been involved with DARPA AQSA for the past four years and have since conducted conceptual and preliminary studies on supersonic transport and recently proposed a patented boom-spike concept to overcome the sonic boom loudness. Gulfstream claims that approximately 35dB reduction is achievable in the loudness levels with advanced shaping and other technologies compared to Concorde. Their design consists of a nose with a retractable spike. The spike's primary purpose is to increase the aircraft's effective length and cause multiple low strength oblique shocks instead of a single strong shock. The spike's size and the position of these spike shocks should be such that they don't coalesce during the pressure signature propagation to the ground. Some quite unsatisfactory aspects of the design are the weight penalty associated with the spike retraction mechanism and the wing swinging mechanism. Hence, further study of stability and aero-elastic issues with detailed wind tunnel tests are needed.

**Other Designs-** Institutions like Boeing, Northrop-Grumman, and IN-RIA are believed to be actively pursuing their designs behind closed doors. Similar Activities are being pursued in Japan and Russia as well.